

# PROCEEDINGS OF SPIE

[SPIDigitalLibrary.org/conference-proceedings-of-spie](https://SPIDigitalLibrary.org/conference-proceedings-of-spie)

## In silico assessment of light penetration into snow: implications to the prediction of slab failures leading to avalanches

Varsa, Petri, Baranoski, Gladimir V.

Petri M. Varsa, Gladimir V. G. Baranoski, "In silico assessment of light penetration into snow: implications to the prediction of slab failures leading to avalanches," Proc. SPIE 11863, Earth Resources and Environmental Remote Sensing/GIS Applications XII, 1186305 (12 September 2021); doi: 10.1117/12.2597638

**SPIE.**

Event: SPIE Remote Sensing, 2021, Online Only

# In silico assessment of light penetration into snow: implications to the prediction of slab failures leading to avalanches

Petri M. Varsa<sup>a</sup> and Gladimir V.G. Baranoski<sup>a</sup>

<sup>a</sup>NPSG, D.R. Cheriton School of Computer Science, University of Waterloo, Waterloo, Ontario, Canada

## ABSTRACT

Snow avalanches are a natural hazard that incur great cost to both property and to human welfare. In some countries they are known to cause more fatalities than both earthquakes and landslides. They also pose a threat to transportation corridors such as year-round highways and railroads that must pass through mountainous regions. There are two categories of avalanche formation that must be recognized when considering slope failure: loose and slab. The former occurs when there is little cohesion in the snowpack and a localized failure progresses downslope. This takes place when the slope angle is steeper than the angle of repose, making failure circumstances comparatively easy to predict. In contrast, slab avalanches occur when a cohesive slab of snow is released over an extended plane of weakness. This happens when a stress, such as the loading of fresh or windblown snow, or the weight of a person, is introduced to a slab layer which has formed on top of a weak layer. The formation of the weak layer that governs slab releases is much more difficult to predict, making this category of avalanche more hazardous. The plane of the weak layer may be comprised of different types of crystals (e.g., hoar and faceted). These are formed either at the surface or at a subsurface depth through morphological processes involving the transport of heat and vapour pressure gradients through the snowpack. These formations are weak since they exhibit poor intergranular bonding and lack shear strength. Even though it has been recognized as a factor in a significant fraction of failure events, the formation of near-surface faceted crystal layers has not been studied extensively. Elucidating the formation of subsurface faceted crystals will advance the current understanding about the formation of snow slabs, which in turn, could be used in the prediction of slope failure. The formation process of subsurface faceted crystals is tied to the penetration of solar radiation into the snowpack. More specifically, absorbed radiation provides the energy that gives rise to the morphological processes governing crystal growth. Consequently, the quantification of light penetration through snow is of interest for studies on the formation of the weak layers associated with snow failure. Despite its importance, investigations of light penetration through snow are still scarce in the literature, and the datasets obtained from field work are affected by experimental limitations. To overcome these limitations and to advance the understanding of light penetration into near-surface layers of snow, we employed a predictive *in silico* experimental setup. Our findings demonstrate that snow grain size and sample density must be carefully accounted for when estimating the quantity of solar radiation contributing to the subsurface morphological processes that form faceted crystals. In addition, our *in silico* experiments provide a detailed assessment of the hyperspectral transmission profiles at different depths. To the best of our knowledge, such an assessment has not been reported in the related literature to date.

**Keywords:** snow, light transport, subsurface, faceted crystals, avalanche

## 1. INTRODUCTION

Snow is a ubiquitous, granular, material that occurs naturally at mid-to-high latitudes. In addition to its impact on the global climate<sup>1</sup> and the availability of potable water during the summer months,<sup>2</sup> seasonal snow also provides an environment for human recreational activity during the winter season.<sup>3</sup> However, the benefits of snowfall do not come without costs. Most specifically, the possibility of avalanches. These natural events incur costs to transportation, damage to property and pose risks to human life.

---

Further author information: (Send correspondence to P.M.V.)

P.M.V.: E-mail: pmvarsa@uwaterloo.ca, Telephone: 1 519 888 4567

G.V.G.B.: E-mail: gvgsbaran@cs.uwaterloo.ca, Telephone: 1 519 888 4567

Earth Resources and Environmental Remote Sensing/GIS Applications XII,  
edited by Karsten Schulz, Proc. of SPIE Vol. 11863, 1186305 · © 2021 SPIE  
CCC code: 0277-786X/21/\$21 · doi: 10.1117/12.2597638

Avalanches are masses of snow that rapidly descend sloped terrain. In fact, they can be classified as a complex type of ground failure<sup>4</sup> involving snow. They are a hazard to human welfare. For instance, they are known to cause more deaths annually in the USA than from other hazards such as earthquakes and landslides.<sup>4</sup> There are also economic consequences incurred by uncontrolled avalanches, notably to the forestry sector and to transportation corridors, which include highways and railways.<sup>5</sup> In addition to the destruction of property, there are great financial losses each year due to delays in transportation.<sup>6</sup> Avalanche detection<sup>7</sup> and prediction can help to minimize these negative consequences. Studying the conditions that affect the release of a snow slab during an avalanche can assist in the development of snow failure predictions.

Avalanches can be categorized as being either wet or dry, depending upon the quantity of moisture in the snowpack,<sup>8</sup> and can be further subdivided into two distinct types of formations. The first type, commonly referred to as loose snow avalanches,<sup>9</sup> are initiated by snow accumulations that lack cohesion. When the slope angle is steeper than the angle of repose, then an avalanche may occur after a localized area of snow exhibits failure and begins to progress downslope. The failure progresses in an inverted V-shape when loose snow encounters additional cohesionless snow in its path. This type of avalanche presents a lower degree of hazard since occurrences are comparatively easy to predict.<sup>4</sup> The second type of avalanche is known as a dry slab avalanche. For this type of avalanche, a cohesive slab of snow on the scale of 10's of meters<sup>10</sup> is released. This cohesive slab rests on top of an extended plane of weakness, which is composed of poorly bonded snow crystals. The slab can be released due to sudden, localized loading, such as from a skier, from gradual, precipitous loading or spontaneously, from changes in the snowpack properties such as warming.<sup>10</sup> The primary difference between the triggering methods is the rate of loading. Upon a triggering event, the stress on a snow slab exceeds the bonding strength of the weak layer that is holding it in place and a catastrophic failure occurs.

As mentioned above, the weak layer is composed of snow crystals with low bonding. The weak layer may form from various types of crystals including surface or depth hoar,<sup>10</sup> graupel or new-fallen low-density stellars,<sup>9</sup> or it may be comprised of near-surface faceted crystals.<sup>9,10</sup> In particular, a significant fraction of slab avalanche accidents are formed with weak failure planes consisting of near-surface faceted crystals.<sup>9,11</sup> After the formation of the weak layer, subsequent snowfalls bury the weak layer and form an upper cohesive slab.

In this work, we focus upon the formation of near-surface faceted crystals, *i.e.*, the formation of a weak layer *before* it is buried by a cohesive surface layer. For near-surface faceted crystals to form, impinging light must penetrate to a depth below the surface of the snowpack. For snowpacks with a sufficient depth, this impinging light is scattered by the grains until it is either reflected or absorbed. The absorbed radiation is the energy source that creates temperature gradients and vapour pressure gradients within the snowpack. These vapour pressure gradients drive the process of snow crystal metamorphism, whereby matter from snow crystals is both vapourized and deposited between crystals as part of the radiation recrystallization process.<sup>9,12</sup> This phenomenon occurs at high elevations where solar radiation is the strongest.<sup>12</sup>

The penetration of solar radiation can be measured directly using a spectrophotometer.<sup>13-16</sup> However, despite current efforts, there are few transmittance datasets available in the literature. Some of these were obtained at locations where impurities were known to affect the sample,<sup>16</sup> which has a significant affect on the spectral characteristics of snowpack.<sup>17</sup> Other datasets were obtained using samples that were morphologically active due to temperature changes.<sup>15</sup> None of these datasets were obtained in high altitude locations where the conditions exist to form weak layers associated with slab avalanches. A lack of such studies may be attributed to the risk of triggering a snow failure event by human loading,<sup>10</sup> or since transmittance measurements are difficult,<sup>18</sup> or because the placement of a measurement device alters the radiation in the vicinity of the sample.<sup>19</sup>

In order to overcome these limitations and contribute to the current knowledge about light penetration in snowpacks, we employed a predictive *in silico* (computational) investigation framework that takes into account the granular nature of snowpacks. By using measured spectral data as a reference and snow characterization parameter values obtained from the literature, we performed experiments investigating the light penetration depth for various snow samples. The experiments were carried out using a first-principles hyperspectral light transport model known as SPLITSnow (*S*Pectral *L*ight Transport model for *S*now).<sup>20</sup> The model takes into account various characteristics of the grains, including the grain size distribution, density and facetness, which are necessary for examining radiative transfer properties within snowpack.

Our experiments investigate the depth to which light penetrates into various snowpack samples by varying individual sample characteristics. To our knowledge, no such investigation has been made available in the literature as of yet.

By elucidating the light penetration depth for various snowpack samples, we hope to assist in the effort of avalanche prediction, thus improving the circumstances governing human safety. In addition to the application of near-surface faceted crystal formation via light propagation, the results of these experiments may also have an impact on other areas such as on the blooming of ice algae<sup>21</sup> and on the radiation budget of shallow lakes.<sup>22</sup>

For the purpose of reproducibility, we have made SPLITSnow available for online use<sup>23</sup> via a model distribution system.<sup>24</sup> Using this system, individuals can execute reflectance and transmittance experiments by specifying the morphological characteristics of the sample using a web interface.<sup>23</sup> Both graphical and numerical results are returned via email to the user for analysis. In addition, we have also provided online access to the supporting data (indices of refraction, *etc.*) used in our investigation.<sup>25</sup>

The remainder of the paper is organized as follows. In Section 2, we briefly summarize the impact that weak layer formation has on the production of dry slab avalanche conditions. In Section 3, we describe the *in silico* framework used to conduct our experiments. In Section 4, we present the results of our experiments and discuss their implications. Finally, in Section 5, we conclude the paper and outline future avenues for research.

## 2. AVALANCHE FORMATION

As mentioned in Section 1, there are two distinct types of dry avalanches. These are loose snow avalanches and dry slab avalanches. Loose snow avalanches occur when the slope angle is steeper than the angle of repose and a small amount of snow becomes unsettled and begins to progress downslope. This type of failure results in a characteristic inverted V-pattern and it is less difficult to predict.<sup>4</sup> Dry slab avalanches are comparatively more difficult to predict. They are identified by the sudden release of a large slab of snow on the scale of 10's of meters across.<sup>10</sup> In this work, we focus on this second type of dry avalanche.

The breakaway fracture point at the top of a dry slab avalanche is known as the crown, the downslope fracture surface, which is usually overridden, is known as the stauwall, and the left and right edges are known as flanks.<sup>26</sup> As already described, the cohesive slab rests on top of a layer of weakly bonded grains such as faceted crystals. Beneath this layer, is a basal layer of snow known as the substratum. This layer remains in place after a failure event. The released slab layer is usually less than one meter thick.<sup>10</sup>

Initiation typically begins with a loading event, whereby a load is added to the surface of the snowpack. This load can be precipitated or wind-blown snow, snow fallen from a higher precipice, or the load of a human participating in a recreational activity such as skiing. The weak layer separates from the slab (and possibly from the substratum) as a localized failure at the point of loading. This localized failure propagates as a shear fracture below the slab in the plane of the weak layer. As a consequence of the shear stress, the large volume of snow contained in the cohesive slab is released as a single formation. The crown and flanks remain after the event and they can be observed after the mass of snow has progressed downslope.

We remark that the weak layer is initially formed either at the existing surface or at a depth just beneath the surface. The formation process may create hoar crystals such as hollow cups or prisms<sup>27</sup> or solid faceted crystals. After formation, the weak layer is buried by further snow accumulation which forms a dangerous cohesive slab. Since a significant fraction of avalanche slabs have a bed surface consisting of faceted crystals,<sup>9,11</sup> we focus the attention of our experiments on the formation of subsurface faceted crystals. In particular, we investigate the light penetration depth of solar radiation since this radiation is the energy source which elicits the morphological processes underlying crystal growth.<sup>12</sup>

## 3. METHODOLOGY AND DATA

Our *in silico* experiments computed the light penetration depth through various natural snow samples. Each sample was selected with distinct characterization values that impact light penetration depth in snowpack. For each sample, a directional-hemispherical transmittance experiment was performed. Prior to the transmittance experiments, we computed the directional-hemispherical reflectance for a sample, and compared the modelled values with measured values obtained from the literature. This baseline comparison enabled us to assess the applicability of the sample characterization datasets that were used in the computation of the transmittance curves.

The measured reflectance curves used for baseline comparisons were obtained from the literature.<sup>28</sup> Although a short description of the sample was provided, a detailed set of snow grain characterization values was not. Using the brief

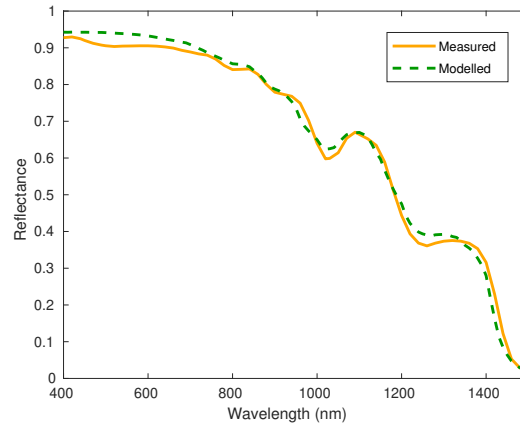


Figure 1. Comparison of measured<sup>28</sup> (orange solid line) and modelled<sup>20</sup> (green dashed line) reflectance curves.

sample description, we deduced a set of characterization values that successfully reproduced the reflectance response. We remark that the deduced values are all within physically valid ranges as reported in the literature.<sup>27</sup>

The SPLITSnow model employs a first-principles simulation whose algorithmic formulation is implemented using an application of Monte Carlo methods<sup>29</sup> and ray optics concepts.<sup>30</sup> Snow grains are generated on the fly in a manner that suits the constraints of the system. To compute the baseline reflectance curve, a uniform distribution was used for the grain size in the range of 300–750  $\mu\text{m}$  with a density of 0.275  $\text{g cm}^{-3}$ . Facetness is a unitless parameter which models the surface details of a grain. It takes values in the range of 0–1, with 1 being the most faceted. This parameter allows for crystalline features to be added to the snow grains by way of microfacets.<sup>31,32</sup> The baseline reflectance curve was computed using a mean facetness of 0.3. The water saturation was set to 5% and the snow temperature was fixed at  $-1^\circ\text{C}$ . The SPLITSnow model shapes snow grains as prolate spheroids. Inscribed circle sphericity<sup>33</sup> is used to relate the prolateness of the grain to a perfect sphere. The spheroidal shape distribution<sup>34</sup> used to compute the baseline reflectance employed a mean sphericity of 0.798 and a standard deviation of 0.064. The sample depth was set to 12 cm and the angle of incidence was set to  $0^\circ$  to match the description of the measured sample.<sup>28</sup>

The SPLITSnow geometrical-optics formulation represents light interaction with the sample using rays that can be associated with any wavelength of light. These ray-sample interactions form the repeated trials of the employed stochastic algorithm. Consequently, the spectral range and resolution are configurable inputs. Our experiments focused on the spectral domain of 400–1500 nm since the constituent components of snow are known to be absorptive in the near infrared domain.<sup>35,36</sup> We remark that this domain includes the values commonly used in studies of light transmittance through snow.<sup>13–16</sup> In our experiments, we considered a spectral resolution of 10 nm. This was sufficient to capture the spectral features present in actual measured data, which was obtained using a coarser resolution.<sup>28</sup>

Fig. 1 presents the comparison between the baseline measured values<sup>28</sup> and modelled values computed using the SPLITSnow model. As it can be observed in the graph, the modelled values are in close agreement with the measured values. The root mean square error between the two curves is 0.02. This indicates a good spectral reconstruction since error values below 0.03 have been described as adequate for remote sensing applications.<sup>37</sup> Accordingly, we employed the same characterization values for our transmittance experiments, varying only the independent variable under test. We will refer to this modelled sample that is characterized by the parameter values used for the baseline comparison as the baseline sample for the remainder of this work.

For our experiments, we selected two characterization parameters to vary, namely grain size and density. The transmittance curves were computed throughout the spectral domain for various depths. For grain size, we selected two average sizes, 0.1 and 0.5 mm, which we label small and medium-sized, respectively. The selected grain size under test is the mean of a uniform distribution of grain sizes, with a range of  $\pm 0.05$  mm. The two density values employed in our experiments are 0.1 and 0.4  $\text{g cm}^{-3}$ , which we label as low and high, respectively. Varying these two characterization parameters yields four study samples. Our experiments were repeated four times for each sample using a selection of sample thicknesses. This approach produced a profile of the light penetration depth for each of the four samples.

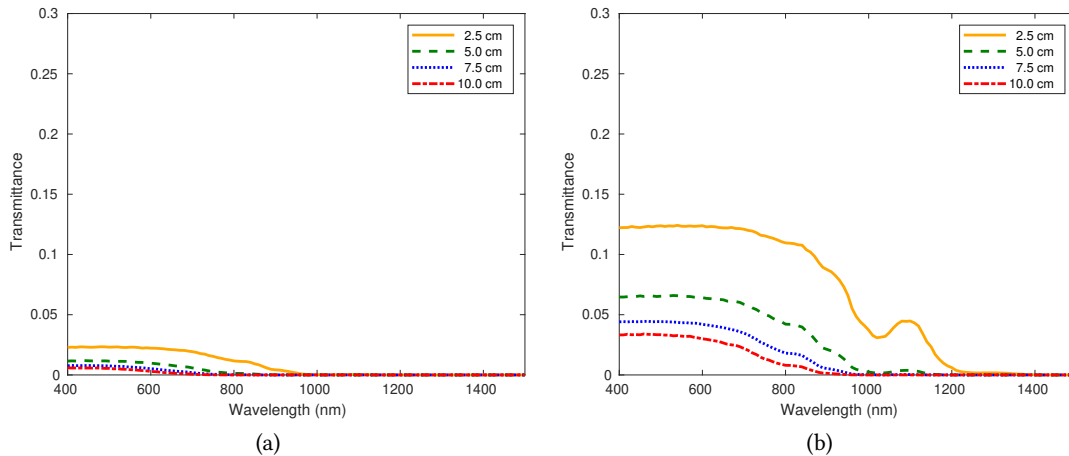


Figure 2. Comparison of modelled transmittance curves computed for two different snow grain sizes for various sample thicknesses. The curves depicted in (a) were computed using an average grain size of 0.1 mm, whereas the curves depicted in (b) were computed with an average grain size of 0.5 mm.

#### 4. RESULTS AND DISCUSSION

In this section, we present the results of our experiments and discuss their implications for remote sensing in the context of weak-layer formation and the prediction of slab avalanches. All transmittance graphs in this section are presented at the same scale. This was done to illustrate the relative impact each independent variable has on the amount of solar energy transmitted through the snowpack.

Our first experiment investigates the effect of grain size on light penetration depth. We computed the transmittances using two different grain sizes. All other characterization parameter values were kept the same as the baseline sample. The data provided in the literature<sup>38</sup> suggest that weak layers contain grains that are 2 mm in size. However, these data were recorded after snow failure. For this investigation, we chose to study small and medium-sized grains, which have not completed the morphological processes induced by solar radiation penetrating the snowpack.

Fig. 2(a) presents graphs of light transmission through the snowpack with small grains (mean size 0.1 mm), whereas Fig. 2(b) presents similar graphs that were generated using medium-sized snow grains (mean size 0.5 mm). Observe that for small grain sizes, less than 3% of solar radiation is transmitted below 2.5 cm depth. However, for medium grain sizes over 10% of solar radiation is transmitted to a depth of 2.5 cm, and nearly 5% is transmitted to a depth of 7.5 cm. This indicates that transmittance is directly proportional to grain size, which is consistent with observations reported in the literature for granular materials.<sup>39-41</sup> Thus, it provides evidence that sufficiently large snow grains will promote the formation of near-surface weak layers, which may lead to the precipitation of avalanches. Indeed, large grain sizes have been observed in the residual weak layer after a failure event.<sup>38</sup>

Our second *in silico* experiment investigates the effect of density on light penetration depth. We computed the transmittances for the baseline sample using two different densities. All other parameter values were kept constant with those of the baseline sample. The low density ( $0.1 \text{ g cm}^{-3}$ ) graphs are presented in Fig. 3(a) and the high density ( $0.4 \text{ g cm}^{-3}$ ) graphs are presented in Fig. 3(b). The low density graphs show a greater transmittance, which is consistent with reports found in the literature.<sup>42,43</sup>

The curves in Fig. 3(a) indicate that a significant fraction of solar radiation penetrates low density snowpacks. At a depth of 2.5 cm, approximately a quarter of the visible light is permeated. The quantity lessens in the infrared, where absorption is more significant. However, the near infrared still shows a non-trivial amount of transmittance, especially in the neighbourhood of 1100 nm. At a depth of 5 cm, less than 15% of solar radiation is transmitted in the visible. Finally, at 10 cm, approximately 7.5% of solar radiation is transmitted.

The transmittance curves in Fig. 3(b) depict the fraction of solar radiation that penetrates through high density snow for various depths. With high density snow, less than 10% of the incident light penetrated below a 2.5 cm depth. At a 10 cm depth, less than 2.5% of the light is transmitted. These findings are consistent with radiation penetration theory

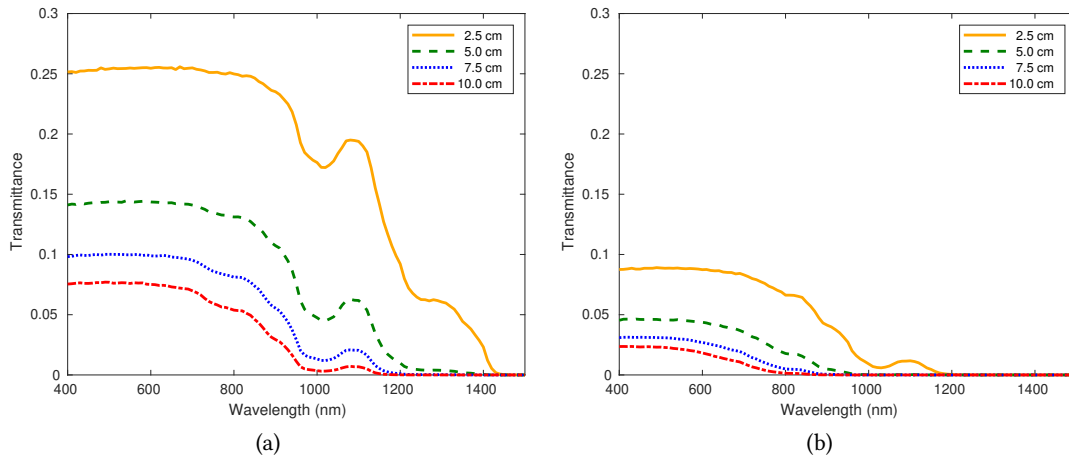


Figure 3. Comparison of modelled transmittance curves computed for two different snow densities for various sample thicknesses. The curves depicted in (a) were computed using a density of  $0.1 \text{ g cm}^{-3}$ , whereas the curves depicted in (b) were computed with a density of  $0.4 \text{ g cm}^{-3}$ .

predicting snow crystal growth,<sup>12</sup> whereby faceted crystal growth is computed to be greatest below the surface at depths less than 15 cm.

Our final experiment addresses the combination of the two independent variables already examined in order to provide insight into light penetration through four distinct study samples. Except for density and grain size, all other parameter values are kept consistent with the baseline sample. The results are presented in Fig. 4. More specifically, the samples used to generate the graphs in the top row were computed using small grains, and the samples used to generate the graphs in the bottom row were computed using medium-sized grains. The samples on the left side were computed using low density snowpacks, and the samples on the right hand side were computed using high density snowpacks. It is interesting to observe that less than 2% of the visible radiation, and only negligible infrared radiation, was transmitted below 2.5 cm for the small grain, high density sample (Fig. 4(b)). In contrast, a significant fraction of both solar and near infrared radiation was transmitted for the the medium-sized grains with low density (Fig. 4(c)).

It is also interesting to make a direct comparison between Figs. 4(a) and (d). Observe that the transmittances are approximately on the same order of magnitude. In Fig. 4(a) the transmittance of the solar radiation is affected by the low density of the snowpack, whereas in Fig. 4(d), the increase in grain size contributes to the quantity of light that is transmitted into the snowpack. A little more than 5% of the visible solar radiation is transmitted to a depth of 2.5 cm in Fig. 4(a) and a little less than 10% of the visible solar radiation penetrates to the same depth in Fig. 4(d). This indicates that both density and grain size are factors that affect the morphological processes that govern the formation of weak layers.

Given the relationship between the penetration of light into snow and the studied grain properties, we conclude that obtaining estimates for both these snowpack properties would assist in the process of avalanche prediction. In particular, low density snowpacks with medium-sized crystals are susceptible to light penetration to a depth that is sufficient to foster the morphological processes that produce weak layers consisting of near-surface faceted crystals. Improved monitoring of snowpacks exhibiting these traits may eventually lead to improved prediction of snow slab failure events.

## 5. CONCLUSION AND FUTURE WORK

Avalanches are natural events incurring significant costs in the form of transportation delays and property damage, while also posing risks to human life.<sup>4-7</sup> We remark that dry slab avalanches are the most hazardous type of these events since they are more difficult to predict. The process of dry slab avalanche formation begins with light impingement on the surface of the snow and the induction of thermal and convective flows below the surface. These morphological processes may produce near-surface faceted crystals of which weak layers are formed. Once buried beneath a cohesive layer, these near-surface faceted crystals form the weak layer associated with slab failure. Although much work has been done to investigate the cause of these failures, works addressing light transmission through snowpack are still scarce

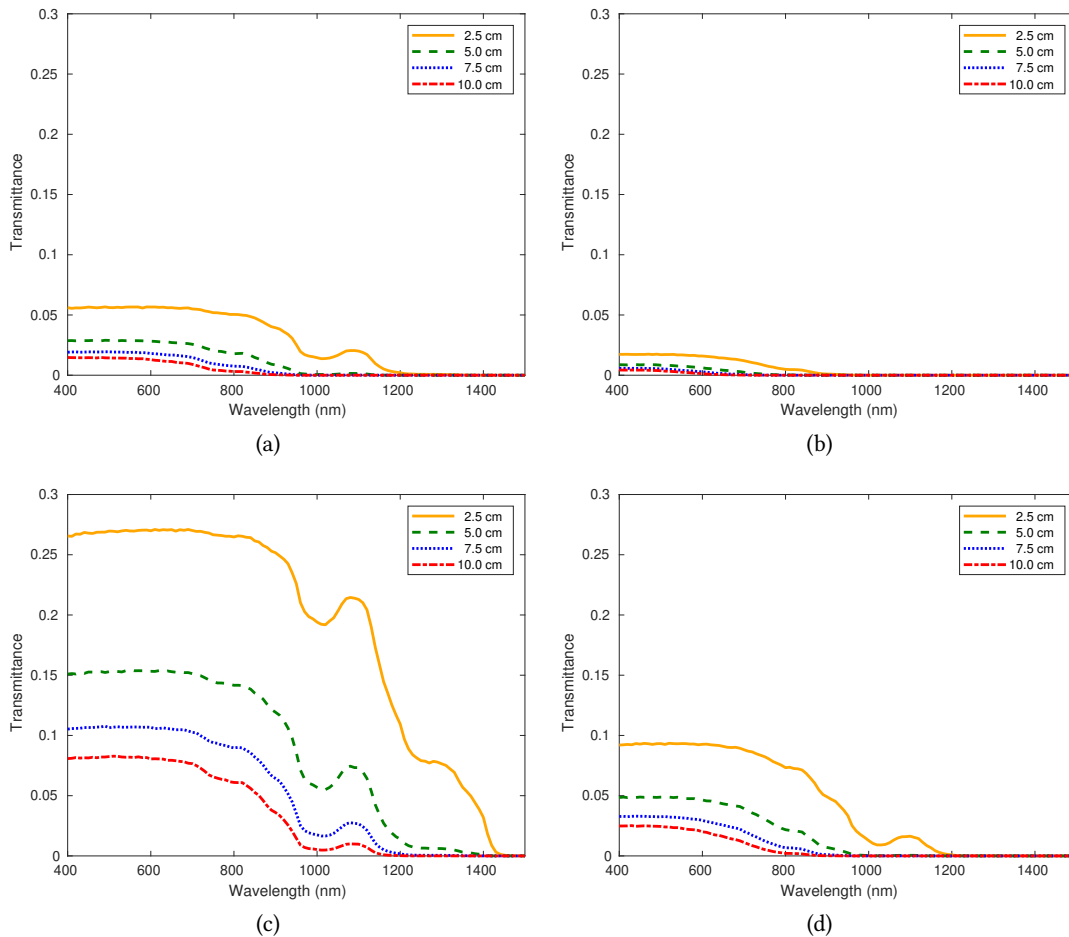


Figure 4. Comparison of modelled transmittance curves computed for four different snow samples for various sample thicknesses. The curves depicted in the top row were generated using small grains (0.1 mm), whereas the curves depicted in the bottom row were generated using medium-sized grains (0.5 mm). The curves depicted on the left were computed using low snow density ( $0.1 \text{ g cm}^{-3}$ ), whereas the curves depicted on the right were computed using high snow density ( $0.4 \text{ g cm}^{-3}$ ).



in the literature. This may be due to the challenging task of accounting for the morphological features at small scales. To address this concern, we performed experiments using an *in silico* investigation approach that is supported by actual measured data and allows for the configuration of the morphological features for various snow samples.

Our findings indicate that the transmittance of a snowpack is proportional to the size of its grains and inversely proportional to its density. Our calculations are also consistent with analytic approaches describing snow crystal growth.<sup>12</sup> More specifically, they demonstrate that particular combinations of grain size and density allow for light to penetrate to the depth required to facilitate near-surface faceted crystal growth in the snow pack. In addition, the results of our investigation strengthen the knowledge required for predictive assessment of the factors leading to snow failure. In turn, such an assessment can be instrumental to the implementation of solutions that reduce the costs incurred from these hazardous events.

The work described in this paper focused on the effect that grain size and density have on light transmission through snowpacks in the formation of weak layers consisting of near-surface faceted crystals. In the future, we intend to expand upon this effort by increasing the quantity of samples that are examined for each trait, thus increasing the dimensionality of each independent variable. This will enable us to investigate the relationship (*e.g.*, linear or quadratic) between the characterization parameter values and their effect on transmittance. This may also add to the understanding of the effect of snow morphology on light penetration through snowpacks. For example, as morphological changes are induced by the impinging light, what is the effect on light penetration throughout the depth of the snowpack, and how is the process of weak layer formation bounded? We also note that other snow grain characterization parameters may have an effect on light transmission through the material. We intend to incorporate other such parameters into our subsequent studies. In particular, we plan to investigate how snow grain facetness may also affect the transmission of light. We note that parameters such as facetness can be effectively studied using a first principles approach such as the one employed in this work.

## ACKNOWLEDGMENTS

This work was supported by the Natural Sciences and Engineering Research Council of Canada (NSERC-Discovery Grant 238337).

## REFERENCES

- [1] Barry, R. G., “The cryosphere and climate change,” in [*Detecting the Climatic Effects of Increasing Carbon Dioxide*], MacCracken, M. C. and Luther, F. M. ., eds., (DOE/ER-0235), ch. 6, 109–148, US Dept. of Energy Washington, DC, Washington, DC (1985).
- [2] Barnett, T., Adam, J., and Lettenmaier, D., “Potential impacts of a warming climate on water availability in snow-dominated regions,” *Nature* **438**(7066), 303 (2005).
- [3] Bielinis, E., Łukowski, A., Omelan, A., Boiko, S., Takayama, N., and Grebner, D. L., “The effect of recreation in a snow-covered forest environment on the psychological wellbeing of young adults: Randomized controlled study,” *Forests* **10**(10), 827 (2019).
- [4] Voight, B., Armstrong, B. R., Armstrong, R. L., Bachman, D., Bowles, D., Brown, R. L., Faisant, R. D., Ferguson, S. A., Fredston, J. A., Kennedy, J. L., Kiusalaas, J., LaChapelle, E. R., McFarlane, R. C., Newcomb, R., Penniman, R., and Perla, R., [*Snow avalanche hazards and mitigation in the United States*], The National Academies Press, Washington, DC, USA (1990).
- [5] Stethem, C., Jamieson, B., Schaerer, P., Liverman, D., Germain, D., and Walker, S., “Snow avalanche hazard in Canada—a review,” *Nat. Hazards* **28**(2), 487–515 (2003).
- [6] Jamieson, B., [*A Synthesis of Geological Hazards in Canada*], ch. Snow avalanches, 75–94, Natural Resources Canada, Ottawa, Canada (2001).
- [7] Patil, A., Singh, G., Kumar, S., Mani, S., Bandyopadhyay, D., Nela, B. R., Musthafa, M., and Mohanty, S., “Snow characterization and avalanche detection in the Indian Himalaya,” in [*Geoscience and Remote Sensing Symposium (IGARSS)*], 2005–2008, IEEE (2020).
- [8] Baggi, S. and Schweizer, J., “Characteristics of wet-snow avalanche activity: 20 years of observations from a high alpine valley (Dischma, Switzerland),” *Nat. Hazards* **50**(1), 97–108 (2009).

- [9] Birkeland, K. W., “Terminology and predominant processes associated with the formation of weak layers of near-surface faceted crystals in the mountain snowpack,” *Arctic Alpine Res.* **30**(2), 193–199 (1998).
- [10] Schweizer, J., Jamieson, J. B., and Schneebeli, M., “Snow avalanche formation,” *Rev. Geophys.* **41**(4) (2003).
- [11] Jamieson, J. B., *Avalanche Prediction for Persistent Snow Slabs*, PhD thesis, The University of Calgary, Calgary, AB, Canada (November 1995).
- [12] Colbeck, S. C., “Snow-crystal growth with varying surface temperatures and radiation penetration,” *J. Glaciol.* **35**(119), 23–29 (1989).
- [13] Dozier, J., Davis, R. E., and Nolin, A. W., “Reflectance and transmittance of snow at high spectral resolution,” in [*Geoscience and Remote Sensing Symposium (IGARSS)*], 662–664, IEEE (1989).
- [14] Beaglehole, D., Ramanathan, B., and Rumberg, J., “The UV to IR transmittance of Antarctic snow,” *J. Geoph. Res.-Atmos.* **103**(D8), 8849–8857 (1998).
- [15] Gerland, S., Liston, G. E., Winther, J.-G., Ørbæk, J. B., and Ivanov, B. V., “Attenuation of solar radiation in Arctic snow: Field observations and modelling,” *Ann. Glaciol.* **31**, 364–368 (2000).
- [16] Perovich, D. K., “Light reflection and transmission by a temperate snow cover,” *J. Glaciol.* **53**(181), 201–210 (2007).
- [17] Warren, S. G. and Wiscombe, W. J., “A model for the spectral albedo of snow. II: Snow containing atmospheric aerosols,” *J. Atmos. Sci.* **37**(12), 2734–2745 (1980).
- [18] Giddings, J. C. and LaChapelle, E., “Diffusion theory applied to radiant energy distribution and albedo of snow,” *J. Geoph. Res.* **66**(1), 181–189 (1961).
- [19] Dunkle, R. V. and Bevans, J. T., “An approximate analysis of the solar reflectance and transmittance of a snow cover,” *J. Meteorol.* **13**(2), 212–216 (1956).
- [20] Varsa, P. M., Baranoski, G. V. G., and Kimmel, B. W., “SPLITSnow: A spectral light transport model for snow,” *Remote Sens. Environ.* **255**, 112272:1–20 (2021).
- [21] Curl, Jr., H., Hardy, J. T., and Ellermeier, R., “Spectral absorption of solar radiation in alpine snowfields,” *Ecology* **53**(6), 1189–1194 (1972).
- [22] Petrov, M. P., Terzhevik, A. Y., Palshin, N. I., Zdorovenov, R. E., and Zdorovenova, G. E., “Absorption of solar radiation by snow-and-ice cover of lakes,” *Water Resour.* **32**(5), 496–504 (2005).
- [23] Natural Phenomena Simulation Group, *Run SPLITSnow Online (Spectrometric Mode)* (2020). <http://www.npsg.uwaterloo.ca/models/splitsnow.php>.
- [24] Baranoski, G. V. G., Dimson, T., Chen, T. F., Kimmel, B. W., Yim, D., and Miranda, E., “Rapid dissemination of light transport models on the web,” *IEEE Comput. Graph.* **32**(3), 10–15 (2012).
- [25] Natural Phenomena Simulation Group, *Snow Data* (2020). <http://www.npsg.uwaterloo.ca/data/snow.php>.
- [26] McClung, D. and Schaerer, P. A., [*The Avalanche Handbook*], The Mountaineers Press, Seattle, WA, USA, 3 ed. (2006).
- [27] Fierz, C., Armstrong, R. L., Durand, Y., Etchevers, P., Greene, E., McClung, D. M., Nishimura, K., Satyawali, P. K., and Sokratov, S., “The international classification for seasonal snow on the ground,” Tech. Rep. 83, UNESCO-IHP, Paris, France (2009).
- [28] Dumont, M., Brissaud, O., Picard, G., Schmitt, B., Gallet, J.-C., and Arnaud, Y., “High-accuracy measurements of snow bidirectional reflectance distribution function at visible and NIR wavelengths – Comparison with modelling results,” *Atmos. Chem. Phys.* **10**(5), 2507–2520 (2010).
- [29] Hammersley, J. M. and Handscomb, D. C., [*Monte Carlo Methods*], Chapman and Hall, London, UK (1964).
- [30] Born, M. and Wolf, E., [*Principles of Optics: Electromagnetic Theory of Propagation, Interference and Diffraction of Light*], Cambridge University Press, Cambridge, UK, 7 ed. (1999).
- [31] Torrance, K. E. and Sparrow, E. M., “Theory for off-specular reflection from roughened surfaces,” *J. Opt. Soc. Am.* **57**(9), 1105–1114 (1967).
- [32] Cook, R. L. and Torrance, K. E., “A reflectance model for computer graphics,” *ACM T. Graphic.* **1**(1), 7–24 (1982).
- [33] Riley, N. A., “Projection sphericity,” *J. Sediment. Res.* **11**(2), 94–95 (1941).
- [34] Vepraskas, M. and Cassel, D., “Sphericity and roundness of sand in coastal plain soils and relationships with soil physical properties 1,” *Soil Sci. Soc. Am. J.* **51**(5), 1108–1112 (1987).
- [35] Palmer, K. F. and Williams, D., “Optical properties of water in the near infrared,” *J. Opt. Soc. Am.* **64**(8), 1107–1110 (1974).
- [36] Warren, S. G. and Brandt, R. E., “Optical constants of ice from the ultraviolet to the microwave: A revised compilation,” *J. Geoph. Res.-Atmos.* **113**(D14), D14220 (2008).

- [37] Jacquemoud, S., Ustin, S., Verdebout, J., Schmuck, G., Andreoli, G., and Hosgood, B., "Estimating leaf biochemistry using PROSPECT leaf optical properties model," *Remote Sens. Environ.* **56**, 194–202 (1996).
- [38] Schweizer, J. and Lüschtg, M., "Characteristics of human-triggered avalanches," *Cold Reg. Sci. Technol.* **33**(2-3), 147–162 (2001).
- [39] Tester, M. and Morris, C., "The penetration of light through soil," *Plant Cell Environ.* **10**, 281 (1987).
- [40] Bänninger, D. and Flühler, H., "Modeling light scattering at soil surfaces," *IEEE T. Geosci. Remote* **42**(7), 1462–1471 (2004).
- [41] Ciani, A., Goss, K., and Schwarzenbach, R., "Light penetration in soil and particulate materials," *Eur. J. Soil Sci.* **56**, 561–574 (2005).
- [42] Woolley, J. and Stoller, E., "Light penetration and light-induced seed germination in soil," *Plant Physiol.* **61**, 597–600 (1978).
- [43] Ollerhead, J., "Light transmittance through dry, sieve sand: Some test results," *Ancient TL* **19**(1), 13–17 (2001).